

## Phase Separation of Asymmetric Binary Hard-Sphere Fluids: Self-Consistent Density Functional Theory

Yaakov Rosenfeld

*Nuclear Research Centre-Negev, P.O. Box 9001, Beer-Sheva 84190, Israel*  
(Received 11 January 1994)

The fundamental-measure free-energy density functional for general inhomogeneous hard-sphere fluids predicts phase separation in bulk binary mixtures with large size ratios,  $R_2/R_1 \geq 4$ , when the packing fractions for the two species are comparable, in qualitative agreement with recent experiments on “nearly hard sphere” colloidal particles. These results open the way, using the same free-energy functional, for studying external field effects (e.g., sedimentation and confining walls) on the entropically driven demixing transition, as encountered in real experiments on colloids.

PACS numbers: 61.20.Gy, 64.70.Ja, 82.70.Dd

Phase separation in a fluid binary mixture of hard spheres is a long standing fundamental problem in statistical mechanics [1], which is the object of renewed theoretical and experimental investigations [2–8]. Fluid phase separation in simple (“atomic”) mixtures is usually induced by *enthalpic* driving forces: steric effects due to nonadditive effective diameters, and van der Waals attractions. The hard-sphere demixing, however, can be driven only by *entropic* effects, and is part of the general question of how phase separation can be induced by purely repulsive interactions [9]. The physical origin of hard-sphere fluid phase separation is the osmotic *depletion effect* [10]: When the surfaces of two large spheres approach within a distance less than the diameter of a small sphere (the small spheres are expelled from between the large ones), the pressure exerted by the small spheres on the outer surfaces is no longer compensated, leading to an effective *attraction* between the large spheres. Ever since Lebowitz and Rowlinson [1] showed that within the Percus-Yevick (PY) closure of the Ornstein-Zernike equations, hard-sphere fluid mixtures are completely miscible for all concentrations and size ratios, it has been generally believed that hard-sphere fluids never phase separate. This was contested recently by Biben and Hansen [2] who found that certain more accurate closures [11] predict phase separation for dense binary hard-sphere fluid mixtures when the size ratio differs considerably from 1, and the partial packing fractions of the two species are comparable. Motivated by this result, the existence of an entropically driven demixing transition was demonstrated in simple, exactly solvable, two-dimensional hard-core lattice models [3,4]. Direct tests of the results from these approximate theories, using numerical simulations of the relevant systems with highly asymmetric size ratios, are precluded, however, by severe ergodicity problems [12] even for a ratio  $R_2/R_1 = 3$ . The hard-sphere demixing is supported by recent experiments on asymmetric “nearly hard sphere” sterically stabilized [6] and charge stabilized [7,8] colloidal suspensions. Bulk phase separation was observed into two disordered phases, and a new ordered phase was found to be located on the cell walls [8]. The

analysis of these experimental results requires a theoretical tool which is able to take into account the effects of external fields, in particular gravity and confining walls.

This Letter offers a new and general theoretical framework for addressing the question of hard-sphere phase separation in external fields, by employing a comprehensive free-energy functional [13] for *inhomogeneous* hard-sphere fluid mixtures. After testing the high accuracy and self-consistency of the model in describing pair correlations for bulk hard-sphere mixtures, I confirm that bulk fluid mixtures of hard spheres are unstable against phase separation for sufficiently asymmetric size ratios, in qualitative agreement with the experimental results on colloidal suspensions. These results open the way (by using the *same* free-energy functional) for studying the entropically driven demixing also for nonuniform hard-sphere fluids and, in particular, for investigating the effects of gravitational settling and confining walls, as encountered in experiments with colloidal particles.

A general powerful method for both uniform and nonuniform fluids is the density functional theory [14]. The central quantity is the excess (over “ideal gas” contributions) free energy,  $F_{\text{ex}}[\{\rho_i(\mathbf{r})\}]$ , a unique functional of the spatially varying one particle densities,  $\{\rho_i(\mathbf{r})\}$ , which originates in interparticle interactions. The density profiles  $\rho_i(\mathbf{r})$  for the fluid subject to external potentials  $u_i(\mathbf{r})$  which couple to the particles of type  $i$  are obtained by solving the Euler-Lagrange equations for the minimization of the grand potential. There is an underlying connection [14] between the structure of the nonuniform fluid and that of the corresponding bulk, uniform fluid, made in the “*test particle limit*” of the density profile equations: When the external potential is obtained by fixing a *test particle* of type  $t$  at the origin,  $u_i(\mathbf{r}) = \phi_{ti}(\mathbf{r})$ , where  $\phi_{ti}(\mathbf{r})$  is the corresponding pair potential between particles of types  $t$  and  $i$  in the fluid, then the density profiles, normalized to unity at large  $r$ , correspond to the pair distribution functions in the bulk uniform fluid  $g_{ti}(\mathbf{r}) = \rho_i(\mathbf{r})/\rho_{i,0}$ , where  $\{\rho_{i,0}\}$  are the average densities of the bulk fluid. The test particle limit of the density profile equations takes the form [13]

$$g_{ii}(r) = \exp\left(-\frac{\phi_{ii}(r)}{k_B T} - \bar{b}_{ii}(r) + \sum_j \rho_{j,0} \int d\mathbf{r}' c_{ij}^{\text{FD}}(|\mathbf{r} - \mathbf{r}'|) h_{ij}(r')\right), \quad (1)$$

where  $h_{ij}(r) = g_{ij}(r) - 1$ , and  $c_{ij}^{\text{FD}}(r)$  are the uniform fluid, bulk limit of the direct correlation functions as obtained from the second functional derivative (FD) of the excess free-energy functional. The *symmetrized* bridge function  $\bar{b}_{ii}(r) = [x_i b_{ii}(r) + x_i b_{ii}(r)]/(x_i + x_i)$  is obtained as the appropriate weighted bulk average of the bridge functions  $b_{ij}(r)$ , which are derived from the *bridge functional*  $B_i[\{\rho_j(\mathbf{r}); \mathbf{r}\}]$  by using  $\rho_i(r) = \rho_{i,0} g_{ii}(r)$ ,

$$b_{ii}(r) = B_i[\{\rho_{j,0} g_{ij}(r)\}; r]. \quad (2)$$

The bridge functional [13] is obtained from the sum of all the terms beyond the second order in the functional Taylor expansion, around the uniform fluid limit, of the excess free-energy functional. The *exact* free-energy functional must obey the “*test particle self-consistency*”: The exact  $g_{ij}(r)$ 's as obtained from the solution of the coupled density profile equations (1) and (2) are identical to those obtained from the Ornstein-Zernike relations,

$$h_{ii}(r) = c_{ii}^{\text{FD}}(r) + \sum_j \rho_{j,0} \int d\mathbf{r}' c_{ji}^{\text{FD}}(|\mathbf{r} - \mathbf{r}'|) h_{ij}(r'). \quad (3)$$

However, given an *approximate* model free-energy functional, it can be *optimized at second order* [13] by *imposing the test-particle self consistency*, i.e., by coupling Eqs. (1) and (2) with Eq. (3). The resulting coupled equations (1)–(3), for *both*  $\{g_{ij}(r)\}$  and  $\{c_{ij}(r)\}$ , in which the bridge functions are obtained from the given, fixed bridge functionals, represent a new method for calculating pair correlations for bulk fluid mixtures. This method is self-consistent [13] with the global application of the same model to the general density profile of inhomogeneous fluids. There is no attempt, however, to impose any specific structural-thermodynamic consistency relations; *everything is predetermined* by the quality of the given free-energy functional.

The present approach employs a free-energy functional for the inhomogeneous hard-sphere fluid mixture which is based on the fundamental geometric measures of the particles [13]. As a special case, this functional derives in a unified way the Percus-Yevick direct correlation functions [1] and the scaled-particle [15] equation of state for the uniform hard-sphere fluid mixture: (a) The uniform (bulk) fluid limit of the model excess free energy is equal to its scaled-particle-theory value for the uniform hard-sphere mixture, corresponding also to the PY “compressibility” equation of state. (b) The second functional derivative of the model functional yields the PY direct correlation functions, i.e.,  $c_{ij}^{\text{FD}}(r) = c_{ij}^{\text{PY}}(r)$ . This free-energy model has already been tested very successfully against computer simulations of density

profiles for a large variety of situations where size or packing effects play an important role [13], but in view of (a) and [1] it does not predict phase separation for bulk hard-sphere mixtures. Using the optimization by the test-particle method [13], as described above, this free energy is presently applied to *bulk* binary mixtures of hard spheres, of radii  $R_1, R_2$  and partial densities  $\rho_{i,0}$  ( $i = 1, 2$ ), with special emphasis on large size asymmetry ( $R_1 \ll R_2$ ) when the packing fractions,  $\eta_i = 4\pi\rho_{i,0}R_i^3/3$ , are comparable ( $\eta_1 \cong \eta_2$  and hence the concentrations obey  $x_2 \ll x_1 \cong 1$ ). Phase separation is signaled by a strong enhancement of concentration fluctuations, leading to the divergence of the long wavelength ( $k \rightarrow 0$ ) limit of the concentration-concentration structure factor,  $S_{cc}(k) = x_1 x_2 [x_2 S_{11}(k) + x_1 S_{22}(k) - 2(x_1 x_2)^{1/2} S_{12}(k)]$ , when the spinodal line is approached; i.e., the Gibbs free energy turns from a concave to a convex function of  $x_1$ ,  $S_{cc}(0) = Nk_B T / (\partial^2 G / \partial x_1^2)_{N,P,T}$ . Defining  $D_c(k) = [1 - \rho_{1,0} \tilde{c}_{11}(k)][1 - \rho_{2,0} \tilde{c}_{22}(k)] - \rho_{1,0} \rho_{2,0} \tilde{c}_{12}(k)$ , then the diagnostic chosen by Biben and Hansen [2] to characterize the spinodal,  $\Lambda \equiv x_1 x_2 / S_{cc}(0) = 0$ , can be equivalently expressed by [16]  $D_c(0) = 0$ , in terms of the  $k \rightarrow 0$  limit of the Fourier transforms of the direct correlations  $\{\tilde{c}_{ij}(k)\}$ . The calculation of the bridge functions from Eq. (2) involves, in our model, only integrations of the density profiles with simple weight functions [13]. Thus, our methods for solving the integral equations and for calculating the spinodals are technically very similar to those described in detail in Ref. [2]. Supplementing the single-component results presented in [13], the present calculations show that our model hard-sphere free-energy functional obeys automatically, and to high accuracy, the whole list of thermodynamic self-consistency requirements also for mixtures, including “virial compressibility,” “zero separation theorem,” “test-particle,” and the “ $b_{ij} = b_{ji}$  symmetry.” Under all conditions which could be checked by simulations, our consistent theory significantly improves on (the already accurate) PY results for the pair correlation functions. The details of these extensive calculations will be published elsewhere. The main results are presented in Fig. 1 where they are compared with other calculations and with experiments on colloids. For any given value of the ratio  $s = R_2/R_1$  the critical pressure  $P_c$ , below which no phase separation occurs, corresponds to the point with the largest value of  $\eta_2$ . For  $s = 10$ , the case considered in detail in Ref. [2], we predict a much higher  $P_c$  ( $P_c^* = 8P_c R_1^3 / k_B T \cong 0.3$  versus  $0.01 < P_c^* < 0.1$ ), corresponding to a much lower critical concentration of the large spheres ( $x_2 \cong 0.002$  versus  $x_2 \cong 0.02$ ), i.e., a *narrow* range,  $\eta_2 < 0.25$ , in comparison with the wide range,

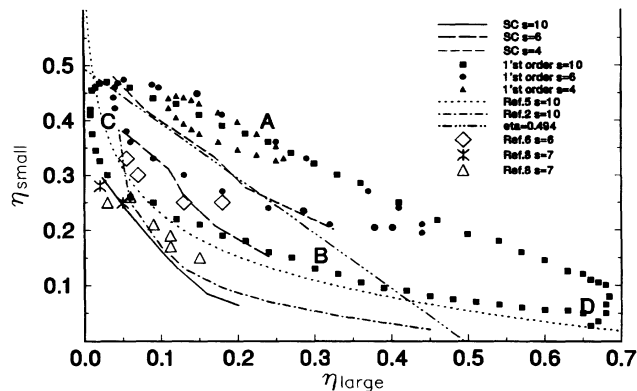


FIG. 1. Theoretical spinodal lines and experimental phase separation results in the  $(\eta_1, \eta_2) \equiv (\eta_{\text{small}}, \eta_{\text{large}})$  plane for different values of the size ratio  $s = R_2/R_1 \geq 1$ . The full, long-dashed, and medium-dashed lines correspond to the self-consistent (SC) density functional theory results for  $s = 10, 6,$  and  $4$  (from bottom to top). The full squares, circles, and triangles are the corresponding results from the present first-order theory. The letters mark the regions of maximum (A), minimum (B), and intermediate (C, D;  $p_C \cong p_D$ ) pressures for  $s = 10$ , as a generic trend for all values of  $s$ . The dotted line represents the solution to Eq. (27) in [5], for  $s = 10$ . The dot-dashed line represents the results of Ref. [2], for  $s = 10$ . The reference triple dot-dashed line,  $\eta = \eta_1 + \eta_2 \cong 0.494$ , marks the  $s = 1$  freezing and serves as a visual aide. The open diamonds represent the  $s \cong 6$  experimental results for silica particles (covering triangles and squares in Fig. 1 of Ref. [6]). The ants and open triangles represent the  $s \cong 7$  experimental bulk phase separation results for polystyrene spheres (same symbols as between the middle and upper lines in Fig. 3 of Ref. [8]).

$\eta_2 < 0.45$ , predicted in Ref. [2]. The “self-consistent” spinodals obey approximately  $\eta = \eta_1 + \eta_2 \cong \text{const.}$  For  $s \leq 4$  the spinodal region for our *fluid* model is in the region where the system is expected to be *solid*, but a phase separation instability of the fluid is predicted by our calculations for  $s \geq 4$ . Like Biben and Hansen, we could not find the second spinodal at higher concentrations of the large spheres.

The depletion attraction of the large spheres, *including* its enhancement [8] close to a wall, is built into the PY closure and into the scaled-particle theory which, nevertheless, predict *no* phase separation. The PY depletion attraction is enhanced by the thermodynamically consistent closures used here and in Ref. [2], enough to produce a spinodal instability. This mechanism becomes clearer through the following simplified density functional calculation. The PY functions are the obvious starting point [recall  $c_{ij}^{\text{FD}}(r) = c_{ij}^{\text{PY}}(r)$ ] for the iterative solution of the self-consistency equations. Inserting  $g_{ij}(r) = g_{ij}^{\text{PY}}(r)$  into the right hand side of Eqs. (2) and (1) we obtain the first-order results  $b_{ij,0}(r)$  and  $g_{ij,0}(r)$ . We observed that the bridge functional is not sensitive to details of the pair functions,  $b_{ij}(r) = b_{ij,0}(r)$ , and noted the slow

variation of the cavity distribution function along the iterations process,  $H_{ij}(r) \equiv h_{ij}(r) - c_{ij}(r) - b_{ij}(r) \cong h_{ij}^{\text{PY}}(r) - c_{ij}^{\text{PY}}(r) - b_{ij,0}(r)$ . From these we obtain the following first-order correction to the Percus-Yevick direct correlations:  $c_{ij}(r) = c_{ij}^{\text{PY}}(r) + [g_{ij,0}(r) - g_{ij}^{\text{PY}}(r)]$ . Inserting this approximation into the diagnostic equation,  $D_c(0) = 0$ , we calculate the corresponding approximation for the spinodal. This approximation can be rewritten as  $\Delta c_{ij}(r) = \Delta g_{ij}(r)$ , and reinterpreted as (e.g.) a mean-spherical approximation,  $\Delta c_{ij}(r) = -\Delta \Phi_{ij}^{(\text{dep})}(r)/k_B T$ , where the additional depletion interactions on top of the reference PY result are evaluated as  $\Delta \Phi_{ij}^{(\text{dep})}(r)/k_B T = -\Delta g_{ij}(r)$ . The unstable regions as encircled by the spinodals from this simplified model (Fig. 1) decrease with decreasing size ratio,  $s = R_2/R_1 = 10, 6, 4$ , and eventually disappear for  $s \cong 3.8$ . Note that the spinodals from the self-consistent theory seem to merge with the first-order results at small packing fractions of the large spheres. The  $s = 10$  results from another semianalytic model [5] partially agree with our first-order density-functional correction to the PY theory (see Fig. 1). In all these models and in Ref. [2], the spinodals are driven by what amounts to *small* corrections (recall that  $x_2 \ll x_1$ , and see, e.g., Fig. 3 in Ref. [5]) to the PY compressibility equation of state. The results are sensitive, however, to the nature of these small corrections, and the accurate prediction of the hard-sphere demixing transition remains a challenging problem.

The self-consistent model and its first-order approximation do not consider the solid at all, and their predictions for the coexisting phase (at higher concentration of the large spheres) are inferred indirectly by comparing the predicted spinodals with the expected region of stability for the fluid phase (roughly indicated by the line  $\eta = \eta_1 + \eta_2 \cong 0.494$  in Fig. 1). The first-order calculations for all size ratios, and the self-consistent results for the relatively small ratios ( $s \leq 5$ ) reinforce the conjecture [5, 17] of a *fluid-solid* phase separation, preempting a fluid-fluid phase separation at a spinodal instability, i.e., coexistence between a solid of high concentration of large spheres, and a low concentration fluid. The self-consistent results for larger ratios ( $s \geq 5$ ) predict a much narrower spinodal range, and thus a corresponding relatively small instability region in the  $(\eta_1, \eta_2)$  plane, favoring a *fluid-fluid* phase separation. The interparticle interactions in the experiments [6–8] are expected to be well represented by hard-sphere potentials. The experiments were done by a straightforward approach: mixing commercially prepared polystyrene particles [8] or custom prepared silica particles [6] of different sizes, and observing them visually over the course of several days. A number of diameter ratios were investigated in [8], and one system with  $s \cong 7$  was explored in detail. Bulk phase separation into two disordered coexisting phases was observed in [8]. The sample separated into upper and lower layers which differed in optical opacity. Phase separation was not

observed in samples with both  $s \lesssim 7$  and  $\eta \lesssim 0.3$ . In [6] only one size ratio of  $s \cong 6$  was considered, and a sudden change of sedimentation velocity with sample concentration signaled the instability. The sediment that was obtained was rather fluid, but the strong gravitational settling of the large spheres makes it very difficult to fully determine the nature of the coexisting phase. The surface crystalline phase reported in [8] was not found in [6] for reasons explained in [8]. The spinodals which we calculated cannot be fully compared with the experimental results because the spinodal does not coincide with the phase transition and because the silica and latex particles are not exactly hard spheres. Bearing this in mind, our self-consistent results for the spinodals provide a reasonably good description (Fig. 1) of the phase separation results and their trends as obtained from these recent experiments on colloidal particles. Our self-consistent model is able to predict the *narrow* range,  $\eta_2 \lesssim 0.2$ , of the phase separation, as found in the experiments, and favors the coexisting fluid phase, as also found experimentally. But of course a much more detailed calculation is required to predict the full phase diagram, the nature of the different phases, and their respective concentrations.

The present study demonstrated the capability of the optimized fundamental-measure free-energy functional to address the interesting question of phase separation in binary hard-sphere mixtures, for which new experimental and theoretical work is just emerging. Further developments within the density functional method are required for enabling a calculation of the phase diagram for confined hard-sphere fluid mixtures, including surface phase separation as described in Ref. [8].

This research was supported by The Basic Research Foundation administered by The Israel Academy of Sciences and Humanities.

- [1] J.L. Lebowitz, Phys. Rev. **133**, A895 (1964); J.L. Lebowitz and J.S. Rowlinson, J. Chem. Phys. **41**, 133 (1964).
- [2] T. Biben and J.P. Hansen, Phys. Rev. Lett. **66**, 2215 (1991); J. Phys. Condens. Matter **3**, F65 (1991).
- [3] D. Frenkel and A.A. Louis, Phys. Rev. Lett. **68**, 3363 (1992).
- [4] J.S. van Duijneveldt and H.N.W. Lekkerkerker, Phys. Rev. Lett. **71**, 4264 (1993).
- [5] H.N.W. Lekkerkerker and A. Stroobants, Physica (Amsterdam) **195A**, 387 (1993).
- [6] J.S. van Duijneveldt, A.W. Heinen, and H.N.W. Lekkerkerker, Europhys. Lett. **21**, 369 (1993).
- [7] S. Sanyal, N. Easwar, S. Ramaswamy, and A.K. Sood, Europhys. Lett. **18**, 107 (1992).
- [8] P.D. Kaplan, J.L. Rouke, A.G. Yodh, and D.J. Pine, Phys. Rev. Lett. **72**, 582 (1994).
- [9] A. de Kijper, B. Smit, J.A. Schouten, and J.P.J. Michels, Europhys. Lett. **13**, 679 (1990); G.I. Kerley, J. Chem. Phys. **91**, 1204 (1989).
- [10] S. Asakura and F. Oosawa, J. Polym. Sci. **33**, 183 (1958).
- [11] F.J. Rogers and D.A. Young, Phys. Rev. A **30**, 999 (1984); P. Ballone, G. Pastore, G. Galli, and D. Gazzillo, Mol. Phys. **59**, 275 (1986).
- [12] P. Fries and J.P. Hansen, Mol. Phys. **48**, 891 (1983).
- [13] Y. Rosenfeld, J. Chem. Phys. **98**, 8126 (1993).
- [14] R. Evans, Adv. Phys. **28**, 143 (1979); in *Inhomogeneous Fluids*, edited by D. Henderson (Dekker, New York, 1992).
- [15] H. Reiss, H. Frisch, and J.L. Lebowitz, J. Chem. Phys. **31**, 369 (1959); H. Reiss, J. Phys. Chem. **96**, 4736 (1992).
- [16] A. Vrij, J. Chem. Phys. **72**, 3735 (1980); X.S. Chen and F. Forstmann, J. Chem. Phys. **97**, 3696 (1992).
- [17] A. Gast, W.B. Russel, and C.K. Hall, J. Colloid. Interface Sci. **109**, 161 (1986).